

1 Comparing Semi-Implicit and Full-Implicit Method for
2 Solving Stiff Density Dependent Diffusion-Reaction
3 Equations Arising in Biofilm Growth Models

4 Hermann J. Eberl and Eric M. Jalbert
5 (heberl@uoguelph.ca, ejalbert@uoguelph.ca)
6 Dept. of Mathematics and Statistics, University of Guelph,
7 Guelph, ON N1G 2W1, Canada

8 **Abstract.** Using the previously established mathematical model for the
9 growth of *Clostridium thermocellum* as an example, a comparison of
10 a semi-implicit and fully-implicit numerical method will be conducted.
11 This example is chosen specifically because it is a stiff problem. The semi-
12 implicit method follows the idea of the semi-implicit Euler method. The
13 fully-implicit method is similar except it computes the solutions multiple
14 times for each time step, each using the newly computed values in place
15 of the solutions at the next time step. These two methods show a minute
16 difference in accuracy, the fully-implicit method being mildly more cor-
17 rect. The difference in computational intensity is more pronounced, the
18 semi-implicit method typically between 3 and 4 times faster. The two
19 values compare nicely and, given the correct situation, both have their
20 uses. Ultimately, the gain in accuracy from the fully-implicit method
21 does generally justify the increase in accuracy; showing the semi-implici
22 method as a sufficient numerical method for these types of problems.

23 **1 Intro**

24 Bacterial biofilms are communities of microorganisms that adhere on immersed
25 aqueous surfaces that can support microbial growth based on the environmental
26 conditions. Biofilms are prevalent on both organic or inorganic surfaces in natu-
27 ral, industrial, or hospital settings. When attached to a surface, these bacteria
28 embed themselves in a self-produced extracellular polymeric substance (EPS).
29 The EPS provides a layer of protection against washout and biocides, making
30 harmful biofilms difficult to remove. This attribute of biofilms is a problem since
31 they are associated with medical issues in the form of, bacterial infections, dental
32 plaque, and other diseases and industrial issues, such as biocorrosion of water
33 pipes. They also contribute positively to wastewater treatment, groundwater pro-
34 tection, soil remediation, and other environmental engineering technologies.

35 To further the understanding of biofilms, a diffusion-reaction model for biofilm
36 growth was proposed in [4]. This model is based on this work.

37 Through the use of some of many established numerical method, an analysis
38 of this biological system can be completed. Typically, in these kind of time-
39 dependent systems, one would discretize both space and time to facilitate ob-
40 taining the solution. The numerical methods can be classified as explicit, semi-
41 implicit, or fully-implicit based on the methods dependence for the state of the
42 system. An explicit numerical method uses the current state of the system to

43 compute the next state while a fully-implicit is the opposite [2]. A semi-implicit
 44 method is specific to a system of differential equations, where at least one equa-
 45 tion is solved using the current state and another is solved using the next state.
 46 This difference between semi-implicit and fully-implicit numerical methods is
 47 that using a fully-implicit method is more computationally heavy, but gives
 48 greater accuracy.

49 2 Model

The specific biology that is discussed here is the growth of *Clostridium thermocellum* biofilms on cellulose sheets. This cellulolytic anaerobic bacteria is a special type of biofilm, it displays uncharacteristic behaviour by not generating a EPS. Based on the work of [3], a simple mathematical model to simulate the growth of *C. thermocellum* can be created. They modelled the biomass density and nutrient concentration as a two PDE-coupled system. Here the spatial diffusion of the nutrient concetration is removed to mimic the carbon substrait that *C.Thermocellum* consumes to grow. The PDE-ODE coupled system is purposed as,

$$M_t = \nabla_x (D(M) \nabla_x M) + f(C, M)M \quad (1)$$

$$C_t = -g(C)M \quad (2)$$

50 where

$$D(M) = \delta \frac{M^\alpha}{(1 - M)^\beta} \quad (3)$$

51

$$f(C, M) = g(C) - \frac{y}{10} \quad (4)$$

52

$$g(C) = \frac{yC}{k + C}. \quad (5)$$

53 The spatial diffusion of biomass M is a density-dependent diffusion, given by
 54 (3). Here, δ depicts the diffusion rate of the biomass. The growth rate of biomass,
 55 $f(C, M)$, is given by (4). The growth rate is Monod kinetic growth with a death
 56 term. There exists a yield term, y , that controls the amount of nutrients the
 57 biomass gains from the substrails. In (2) there is only a consumption term from
 58 the bacteria consuming the carbon substrait. Emphasis will be made to point
 59 out that (2) does not have spatial dependencies, since the cellulose sheet is a
 60 solid fiber that cannot move.

⁶¹ **2.1 Nondimensionalization**

For this system, it is better to nondimensionalize. To do this, the following variable changes are used:

$$x = \frac{\chi}{L} \implies Ldx = d\chi \quad (6)$$

$$t = \mu\tau \implies \frac{1}{\mu}dt = d\tau \quad (7)$$

$$C = \frac{\bar{C}}{C_0} \quad (8)$$

$$\delta = \frac{1}{\mu L^2} \bar{\delta} \quad (9)$$

$$k = \frac{\bar{k}}{C_0} \quad (10)$$

$$\nu = \frac{\bar{\nu}}{\mu C_0} \quad (11)$$

$$\mu = \bar{\mu} \quad (12)$$

This gives the system

$$M_t = \frac{1}{\mu L^2} \nabla_x \left(\hat{D}(m) \nabla_x M \right) + \frac{1}{\mu} \hat{f}(C, M) \quad (13)$$

$$C_t = \frac{-1}{C_0 \mu} \hat{g}(C, M) \quad (14)$$

⁶² where

$$\hat{D}(M) = \mu L^2 \delta \frac{M^\alpha}{(1 - M)^\beta} \quad (15)$$

$$\hat{f}(C, M) = \frac{\mu C C_0}{k C_0 + C C_0} M \left(1 - \left(\frac{M}{C} \frac{M_0}{C_0} \right)^\gamma \right) \quad (16)$$

$$\hat{g}(C, M) = -\frac{\mu C_0 \nu C C_0}{k C_0 + C C_0} M \quad (17)$$

⁶³ This can be greatly simplified by cancelling out parameters.

$$M_t = \nabla_x \left(\delta \frac{M^\alpha}{(1 - M)^\beta} \nabla_x M \right) + \frac{C}{k + C} M \left(1 - \left(\frac{M}{C} \frac{M_0}{C_0} \right)^\gamma \right) \quad (18)$$

$$C_t = -\frac{\nu C}{k + C} M \quad (19)$$

⁶⁴ Now we can name functions and get the final nondimensionalized system.

$$M_t = \nabla_x (D(M) \nabla_x M) + f(C, M) \quad (20)$$

$$C_t = -g(C, M) \quad (21)$$

65 where

$$\begin{aligned} D(M) &= \delta \frac{M^\alpha}{(1-M)^\beta} \\ f(C, M) &= \frac{C}{k+C} M \left(1 - \left(\frac{M}{C} \frac{M_0}{C_0} \right)^\gamma \right) \\ g(C, M) &= \frac{\nu C}{k+C} M \end{aligned} \quad (22)$$

66 This system is solved on a non-dimensionalized square region $\Omega \in [0, 1] \times$
67 $[0, 1]$. On this region, there are Neumann boundary conditions defined as

$$\frac{\partial M}{\partial x} = \frac{\partial C}{\partial x} = 0, \quad \text{on } \partial\Omega. \quad (23)$$

68 3 Method

69 There are three main aspects to the numerical method of solving this system.
70 The system must be temporally and spatially discretized, then a solution for C
71 and M can be computed using numerical methods.

72 For the solution of C , since it has no spatial diffusion, a simple application
73 of the Trapezoidal rule can be used. The idea is to integrate both sides of (2) to
74 get,

$$C^{t_{n+1}} - C^{t_n} = \frac{t_{n+1} - t_n}{2} (g(C^{t_{n+1}}, M^{t_{n+1}}) + g(C^{t_n}, M^{t_n})). \quad (24)$$

75 By rearranging (24) and subbing in (5) an equation explicitly for $C_{t_{n+1}}$ is found.
76 This solution gives two values for $C_{t_{n+1}}$ since it is solved using the quadratic
77 formula. Only the positive branch of the quadratic formula is relevant to this
78 problem, since the negative branch behaves unrealistically.

79 The solution of M is more involved, because of the density-dependent diffusion
80 term. This means that it must be spatially discretized as well as temporally
81 discretized. The spatial discretization of the system is a simple application of
82 the finite difference method. Following the example of finite differences for 2-D
83 problems as described in [6] a grid is created to approximate each point using a
84 five-point stencil. Here, the values at the boundaries are unknown and as such
85 are also included in the five-point stencil. These boundary points are computed
86 using a second order approximation. The temporal discretization is a forward difference
87 between the current and next time step. Applying these discretizations

88 to (1) and rearranging gives a system of linear equation defined by,

$$\begin{aligned} \frac{M_{i,j}^n}{\Delta t} &= \frac{-D_{i,j-\frac{1}{2}}^n}{\Delta y^2} \cdot M_{i,j-1}^{n+1} + \frac{-D_{i-\frac{1}{2},j}^n}{\Delta x^2} \cdot M_{i-1,j}^{n+1} \\ &+ \left[\frac{D_{i,j-\frac{1}{2}}^n}{\Delta y^2} + \frac{D_{i-\frac{1}{2},j}^n}{\Delta x^2} + \frac{D_{i+\frac{1}{2},j}^n}{\Delta x^2} + \frac{D_{i,j+\frac{1}{2}}^n}{\Delta y^2} - f(C^n, M^n) + \frac{1}{\Delta t} \right] \cdot M_{i,j}^{n+1} \\ &+ \frac{-D_{i+\frac{1}{2},j}^n}{\Delta x^2} \cdot M_{i+1,j}^{n+1} + \frac{-D_{i,j+\frac{1}{2}}^n}{\Delta y^2} \cdot M_{i,j+1}^{n+1}, \end{aligned} \quad (25)$$

89 where $M_{i,j}^n = M^{t_n}(x_i, y_j)$, $D_{i,j}^n = D(M_{i,j}^n)$, and (x_i, y_j) is the ordered pair at
90 grid point i, j .

91 Using (25) a five-diagonal block matrix can be created, defined as,

$$A = \begin{pmatrix} M_{i,j} & M_{i+1,j} & & M_{i,j+1} & & & \\ M_{i-1,j} & \ddots & \ddots & & \ddots & & \\ & \ddots & \ddots & \ddots & & \ddots & \\ M_{i,j-1} & & M_{i-1,j} & M_{i,j} & M_{i+1,j} & & M_{i,j+1} \\ & \ddots & & \ddots & \ddots & \ddots & \ddots \\ & & M_{i,j-1} & & M_{i-1,j} & M_{i,j} & M_{i+1,j} & M_{i,j+1} \\ & & & \ddots & & \ddots & \ddots & \ddots \\ & & & & \ddots & \ddots & \ddots & M_{i+1,j} \\ & & & & M_{i,j-1} & & M_{i-1,j} & M_{i,j} \end{pmatrix}, \quad (26)$$

92 where each $M_{i,j}$ is the coefficient based on (25).

93 The solving of (26) can be completed through use of a linear solver. According
94 to [1], if (26) is positive definite and symmetric then it can be solved using the
95 Conjugate Gradient method.

96 **Proposition 1.** *The matrix A, defined in (26), is positive definite and symmetric.*

98 *Proof.* Matrix A is positive definite if all the eigenvalues are positive. Using
99 Geršgorin's circle theorem, see [5], the eigenvalues can be shown to be positive
100 if, on all rows independently, the sum of the off-diagonals values are less than
101 the diagonal value. Mathematically we have,

$$\begin{aligned} &\left| \frac{-D_{i,j-\frac{1}{2}}^n}{\Delta y^2} + \frac{-D_{i-\frac{1}{2},j}^n}{\Delta x^2} + \frac{-D_{i+\frac{1}{2},j}^n}{\Delta x^2} + \frac{-D_{i,j+\frac{1}{2}}^n}{\Delta y^2} \right| \\ &< \left| \frac{D_{i,j-\frac{1}{2}}^n}{\Delta y^2} + \frac{D_{i-\frac{1}{2},j}^n}{\Delta x^2} + \frac{D_{i+\frac{1}{2},j}^n}{\Delta x^2} + \frac{D_{i,j+\frac{1}{2}}^n}{\Delta y^2} - f(C^n, M^n) + \frac{1}{\Delta t} \right|, \end{aligned} \quad (27)$$

102 which simplifies to,

$$f(C_{i,j}^n, M_{i,j}^n) < \frac{1}{\Delta t}, \quad (28)$$

103 which is true give the values of Δt that are used. Therefore we have that A is
104 positive definite.

The symmetry of A can be trivially shown if one considers the formation of the diagonals. On a single row, each element corresponds to the adjacent grid points of grid i, j . As the grid ordering counts along, the elements that are equidistance from the diagonal are actually reference to the same grid point. Therefore we have symmetry. \square

105 Given that A is positive definite and symmetric, the conjugate gradiant
106 method can be used to compute the solution. As an added property, A also
107 happens to be diagonally dominate. This means that it could be solved using
108 Bi-Conjugate Gradient Method. However the Conjugate Gradient method has a
109 faster computation time then Bi-Conjugate Gradiant method for this problem
110 and is used for this reason [1].

111 Now that the method for solving C and M have been discussed, the method
112 for solving the system as a whole can be investigated. Since $M^{t_{n+1}}$ only depends
113 on C^{t_n} and M^{t_n} while $C^{t_{n+1}}$ depends on C^{t_n}, M^{t_n} , and $M^{t_{n+1}}$ the solution
114 for M should be computed first and then it can be used to compute C . This
115 idea is translated into Algorithm 1 to be the fully-implicit method for solving
116 the system. The semi-implicit method for solving the system is the same as
117 Algorithm 1 but with $eSoln = 0$, forcing only a single iteration of the loop.

```

Data:  $M_{prev}$  and  $C_{prev}$  is previous timestep solutions
begin
    while  $diffC > eSoln$  and  $diffM > eSoln$  do
        Solve for  $M^{i+1}$  using  $C^i$  and  $M_{prev}$ ;
        Solve for  $C^{i+1}$  using  $C_{prev}$ ,  $M^{i+1}$ , and  $M_{prev}$ ;
        Let  $diffC = (C^{i+1} - C^i)$ ;
        Let  $diffM = (M^{i+1} - M^i)$ ;
        Let  $C^i = C^{i+1}$  Let  $M^i = M^{i+1}$ ;
    end
end

```

Algorithm 1: Algorithm for the fully-implicit solving of (1-2).

118 4 Results

119 4.1 Simulation Setup

120 All the simulations were run on a custom built workstation with an Intel Xeon
121 CPU E5-2650 (1.2 GHz, 20 MB cache size) and 32 GB RAM under Red Hat
122 Enterprise Linux Server release 6.5 (Santiago). Running the simulations with
123 OpenMP, took advantage of the 16 processors of the Intel Xeon CPU, each with
124 2 threads. The GNU fortran compiler version 4.4.7 was used for the typical
125 simulation results; compiler arguments were

```
126 -O3 -fdefault-real-8 -fopenmp .
```

127 The Intel Fortran compiler version 14.0.2 was used for the speed results; compiler
128 arguments were

```
129 -O3 -r8 -openmp .
```

130 The simulations were solved on a 1024×1024 grid, using $\Delta t = 10^{-2}$.

131 4.2 Results

132 Using the parameter values defined in the Appendix, the simulation was run
133 and the results were as shown in Figure 1.

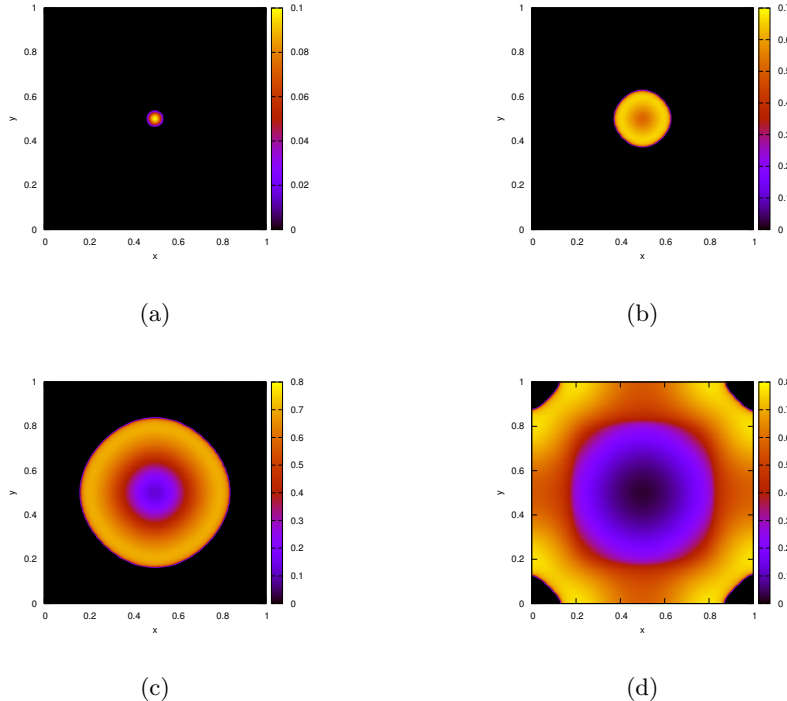


Fig. 1. Typical simulation using parameters from Appendix at (a) $t = 0$, (b) $t = 10$,
(c) $t = 20$, (d) $t = 30$

134 **4.3 Comparisons**

135 A comparison of the two methods can be done by looking at both their
 136 computation time and the accuracy of the solution. The computation time is
 137 computed by the system clock from the start of the algorithm to the end of
 138 the algorithm. The accuracy of the solution can be found by computing the
 139 normed-difference between two solutions, as follows,

$$\epsilon_{sol} = \frac{\|u_1 - u_2\|}{\|u_1\|} \quad (29)$$

140 Two comparisons will be done with the norm. One with the solution at the
 141 current grid size and the solution at the next smallest grid size. This is because,
 142 the smaller the grid refinement, the more accurate the solution. Thus to compare
 143 the accuracy of methods, this will be used. The other will be with the solution
 144 and the solution with the smallest $eSoln$, as defined in Algorithm 1. These two
 145 comparison will provide two difference measures of the accuracy of the method.

146 The other comparison will be with where the method is spending its time.
 147 The fully-implicit method should have less iterations of the linear solver. Thus
 148 with will be measured as *Iteration2*. *Iterations1* is the number of iterations
 149 between solving M and C , according to Algorithm 1.

150 The results of the method comparison can be seen in Tabel 1.

Tol. 1	Computation Time	ϵ_{sol}	Avg. Iter. 1	Max Iter. 1	Avg. Iter. 2	Max Iter. 2
10^0	1430.05	—	1	1	44.08	72
10^{-2}	—	—	—	—	—	—
10^{-4}	—	—	—	—	—	—
10^{-8}	—	—	—	—	—	—

Table 1. Results from running simulation with different Tolerance 1 values. Note,
 Tolerance 1 of 10^0 is the semi-implicit method.

151 **5 Conclusions**

152 The numerical simulating of this problem can be solved in many different
 153 manners. Using the fully-implicit method as described in Algorithm 1 allows for
 154 an extra degree of accuracy for the solution. That being said, the difference in
 155 computation time is not necessarily worth the increased workload. The semi-
 156 implicit method has shown to provide solution that are sufficiently accurate and
 157 thus the extra computations for the fully-implicit method are not always needed.
 158 The choice of method is mostly dependent on the problem that is being solved
 159 and the required accuracy of the solution. With powerful computers becoming
 160 more readily available, the sacrifice of computation speed becomes a smaller
 161 price.

162 **Appendix**

Variable/Parameter	Dimensions	Parameter Value
x	[days]	—
t	[meters]	—
M	[—]	—
C	[$\frac{\text{grams}}{\text{meters}^3}$]	—
δ	[$\frac{\text{meters}^2}{\text{days}}$]	10^{-12}
α	[—]	4
β	[—]	4
y	[days $^{-1}$]	6
k	[$\frac{\text{grams}}{\text{meters}^3}$]	4

Table 2. List of parameters and their dimensions

163 **References**

- 164 1. R. Barrett, M. Berry, Chan T.F., J. Demmel, J. Donato, J. Dongarra, V. Eijkhout, R. Pozo, C. Romine, and H. van der Vorst. *Templates for the Solution of Linear Systems: Building Blocks for Iterative Methods*. Society for Industrial and Applied Mathematics, 1st edition, 1987.
- 165 2. J.C. Butcher. *Numerical Methods for Ordinary Differential Equations*. Wiley, 2nd edition, June 2008.
- 166 3. A. Dumitrashe. *Understanding Biofilms of Anaerobic, Thermophilic and Cellulolytic Bacteria: A Study towards the Advancement of Consolidated Bioprocessing Strategies*. PhD thesis, University of Toronto, 2014.
- 167 4. H.J. Eberl, D.F. Parker, and van Loosdrecht M.C.M. A new deterministic spatio-temporal continuum model for biofilm development. *Journal of Theoretical Medicine*, pages 161–175, 2001.
- 168 5. Geršgorin S. über die abgrenzung der eigenwerte einer matrix. *Bulletin de l'Académie des Sciences de l'URSS. Classe des sciences mathématiques et na*, pages 749–754, 1931.
- 169 6. Y. Saad. *Iterative Methods for Sparse Linear Systems*. Society for Industrial and Applied Mathematic, 2nd edition, 2003.
- 170
- 171
- 172
- 173
- 174
- 175
- 176
- 177
- 178
- 179
- 180